AquaTechnica 6(2): 109-120 (2024)
ISSN 2737-6095
DOI https://doi.org/10.33936/at.v6i2.6893
https://doi.org/10.5281/zenodo.13357643

AquaTechnica

Ultrastructure of spermatogenesis in lion's paw scallop *Nodipecten subnodosus* (G. B. Sowerby I, 1835), with some implications in the systematics of the Pectinidae

Ultraestructura de la espermatogénesis de la almeja mano de león *Nodipecten subnodosus* (G. B. Sowebry I, 1835) con algunas implicaciones en la sistemática de los Pectinidae

Marco A. Ángel-Dapa[1], Marcial Arellano-Martínez[1], Ether Uría-Galicia[2], Edgar O. López-Villegas[2], Bertha P. Ceballos-Vázquez[1], Pedro E. Saucedo[3]
[1]Instituto Politécnico Nacional, Centro Interdisciplinario de Ciencias Marinas (CICIMAR), Av. Instituto Politécnico Nacional s/n Col. Playa Palo de Santa Rita. C.P. 23096, La Paz, B.C.S. México.
[2]Instituto Politécnico Nacional, Escuela Nacional de Ciencias Biológicas. Unidad Profesional Lázaro Cárdenas, Prolongación de Carpio y Plan de Ayala s/n, Col. Santo Tomas, C.P. 11340, Delegación Miguel Hidalgo, Ciudad de México.
[3]Centro de Investigaciones Biológicas del Noroeste (CIBNOR). Av. Instituto Politécnico Nacional 195, Col. Playa Palo de Santa Rita Sur, La Paz, B.C.S., 23096, México.
Correspondencia: *Pedro E. Saucedo* ***E-mail:*** *psaucedo04@cibnor.mx*

Original article | Artículo original

Keywords
Scallops
reproduction
spermatogenesis
taxonomy

ABSTRACT | This is the first study to characterize the ultrastructure of spermatogenesis in the lion's paw scallop *Nodipecten subnodosus*, discussing some implications of cell morphology and function in the systematics of the family Pectinidae. Gonad samples were collected on a monthly basis during an annual cycle and processed using conventional TEM techniques. The number and area of developing cells occurring throughout spermatocytogenesis, meiosis, and spermiogenesis were determined. Overall, the arrangement of developing cells was concentric and most cellular changes comprising the transition from spermatogonia to spermatid matched the general pattern of marine bivalves undergoing external fertilization. The main features included a primitive-type, tailed sperm with four spherical mitochondria located in the midpiece, and the typical 9+2 arrangement of microtubules surrounding the centriole. During spermatogenesis, the key changes in cell morphology occurred up to the spermatozoon stage, including the appearance of a bullet-shaped nucleus, a conical acrosome, a small oval-shaped proacrosomal vesicle, and two lateral satellite fibers linked to the centriole. The flagellum also formed up to the sperm stage. Taxonomically, these features appear to be family-specific or species-specific and suggest that *N. subodosus* may be closely related to the hermaphrodite scallops *Patinopecten yessoensis*, *Chlamys farreri farreri*, *C. swiftii*, and *Argopecten irradians* within the family Pectinidae.

Palabras clave
Vieira
reproducción
espermatogénesis
taxonomía

RESUMEN | Este es el primer estudio que caracteriza la ultraestructura de la espermatogénesis en la almeja mano de león *Nodipecten subnodosus*, discutiendo algunas implicaciones de la morfología y función celular en la sistemática de la familia Pectinidae. Se recolectaron muestras de gónadas mensualmente durante un ciclo anual y se procesaron utilizando técnicas MET convencionales. Se determinó el número y el área de células en desarrollo que se presentaron durante la espermatocitogénesis, la meiosis y la espermiogénesis. En general, la disposición de las células en desarrollo fue concéntrica y la mayoría de los cambios celulares que comprenden la transición de espermatogonias a espermátidas coincidieron con el patrón general de los bivalvos marinos sometidos a fertilización externa. Las características principales incluían un espermatozoide con cola de tipo primitivo con cuatro mitocondrias esféricas ubicadas en la pieza intermedia y la típica disposición de microtúbulos 9+2 que rodean el centríolo. Durante la espermatogénesis, los cambios clave en la morfología celular ocurrieron hasta la etapa de espermatozoide, incluida la aparición de un núcleo en forma de bala, un acrosoma cónico, una pequeña vesícula proacrosomal de forma ovalada y dos fibras satélite laterales unidas al centríolo. El flagelo también se formó hasta la etapa de esperma. Taxonómicamente, estas características parecen ser específicas de una familia o de una especie y sugieren que *N. subodosus* puede estar estrechamente relacionado con las vieiras hermafroditas *Patinopecten yessoensis*, *Chlamys farreri farreri*, *C. swiftii* y *Argopecten irradians* dentro de la familia Pectinidae

Recibido: 15-07-2024 | **Aprobado:** 12-08-2024 | **Versión final:** 18-08-2024

Universidad Técnica de Manabí
Fundado en 1952

INTRODUCTION

In recent decades, the increasing resolving power of electron microscopy has made it possible to characterize many morphological and functional aspects of gametogenesis in different species of commercially-valuable marine bivalves. Among some of the earliest basic studies, those on the king scallop *Pecten maximus* (Dorange and Le Pennec 1989), black-lip pearl oyster *Pinctada margaritifera* (Thielley *et al*. 1993), eastern oyster *Crassostrea virginica* (Eckelbarger and Davis 1996), and penshell *Pinna nobilis* (De Gaulejac *et al*. 1995) allowed the identification and description of cell types, organelles, and structures involved in key aspects of gametogenesis. In turn, this knowledge helped to understand the relationship between gonad condition (e.g. synthesis, storage and allocation of energy reserves; differentiation, development, ripeness, release, and final reabsorption of gametes) and larval viability and condition (e.g. survivor, growth, recruitment).

With spermatogenesis in particular, recent research has focused on analyzing the taxonomic value of sperm morphology, acrosome origin and structure, and mitochondrial arrangement to elucidate the family- or species-specific features associated with the life cycles of closely related species. Some of these studies have been conducted with the black ark *Anadara tuberculosa* (Ortíz *et al*. 2003), white clam *Chione californiensis* (Ortiz *et al*. 2006), Manila clam *Ruditapes philipinarum* (Kim *et al*. 2013), penshell *Atrina maura* (Camacho-Mondragón *et al*. 2014), and Pacific spiny oysters *Spondylus calcifer* and *S. princeps* (Villalejo-Fuerte *et al*. 2018). For other commercially-valuable bivalve mollusks, such as pectinid scallops, this taxonomic approach is important given the lack of information relative to the ultrastructure of spermatogenesis (Table 1).

Table 1. Comparative morphology and structure of spermatozoon in five Pectinidae scallops (Kim 2001; Jun *et al*. 2012).
Tabla 1. Morfología y estructura comparadas del espermatozoide en cinco miembros de la familia Pectinidae (Kim 2001; Jun *et al*. 2012).

Species	Sperm	Head				Acrosome		Midpiece	Satellite	Reference
	Size (µm)	Nucleus Morphology	Nucleus length (µm)	Nucleus width (µm)	Shape	Length (µm)	Width (µm)	(# Mit)		
Patinopecten yessoensis	3.48	Vase	2.90	1.48	Cone	0.60	0.12	4	Present	Kim 2001
Argopecten irradians	2.27	Jar (bullet)	1.44	1.38	Cone	0.33	0.12	5	Present	Kim 2001
Chlamys farreri fareri	3.68	Vase	2.75	1.13	Cone	0.50	0.14	4	Present	Kim 2001
Chlamys swifti	3.81	Vase	2.6	1.41	Long cone	0.63	0.12	4	Present	Jun *et al*. 2012
N. subnodsus	2.49	Bullet	1.50	1.40	Cone	0.56	0.13	4	Present	**Present study**

Mit = Mitochondria

The lion's paw scallop *N. subnodosus* (G. B. Sowerby I, 1835) is one of the largest members of the family Pectinidae; it is distributed from the Gulf of California to Peru, but finds its greatest potential for commercial cultivation in the middle part of the Baja California Peninsula (Maeda-Martínez and Lodeiros 2011, Angel-Dapa *et al*. 2015). Here, the species has been extensively fished for human consumption, due to the large size, soft texture, and appealing flavor of its adductor muscle (Beltrán-Lugo *et al*. 2006). However, other problems associated with the lack of planning of aquaculture-based programs and spread of new pathogenic diseases have caused many natural stocks of the species to gradually deplete or disappear in many sites of the Baja California Peninsula (Maeda-Martínez and Lodeiros 2011, Angel-Dapa *et al*. 2015). However, few aspects of the species' reproduction for population recovery purposes have been studied to date, and most have focused on the conditioning of broodstock with different diets and temperatures (Gutiérrez-Villaseñor and Chi-Barragán 1997), growth and gametogenesis (Arellano-Martínez *et al*. 2004a), gross chemical composition of the gonad and somatic tissues during gametogenesis (Arellano-Martínez *et al*. 2004b), and changes in fatty acid, sterol, and monoamine composition (Palacios *et al*. 2005, 2007, López-Sánchez *et al*. 2009).

The present study characterized the ultrastructure of spermatogenesis in *N. subnodosus* aimed to identify the type, size, and main role of cells and organelles involved in sperm maturation. The implications of some of these features for the systematics of the species within the family Pectinidae are discussed.

MATERIALS AND METHODS

Fifteen *N. subnodosus* adults (130 ± 10 mm shell height) were collected every month during an annual cycle at Bahía Tortugas, Baja California Sur, Mexico (27°41'29" N; 114°53'12" W). After measuring (0.1 mm) and weighing (0.1 g) each scallop, samples of six male gonads covering each developmental stage were excised, fixed in 2.5% glutaraldehyde, washed in 2.5% sodium phosphate buffer, and postfixed in osmium tetroxide (Camacho-Mondragón *et al*. 2014). The samples were then dehydrated in an ascending series of ethanol concentrations, infiltrated in a 1:1 solution of propylene oxide and epoxy resin, and embedded in Epon 812 (Electron Microscopy Sciences, Hatfield, PA). Ultra-thin sections (70 nm) were mounted on copper grids, contrasted with uranyl acetate and lead citrate, and observed under a transmission electron microscope (JEOL-100SX; JEOL Inc, Peabody, MA).

Spermatogenesis was characterized according to the three phases proposed by Ortíz *et al*. (2003, 2006): (1) Spermatocytogenesis; (2) Meiosis; and (3) Spermiogenesis. In each case, the number, area (μm^2), and location of all developing cell types (spermatogonia, primary and secondary spermatocytes, spermatids, and spermatozoa) were calculated. For mature spermatozoa, aspects such as the morphological features of acrosome length (e.g. linear distance from its posterior edge to the posterior edge of nuclear invagination), the area and length of the nucleus (linear distance from the posterior edge of the invagination to the anterior edge of the midpiece), and the cytoplasm-nucleus ratio were measured. All these calculations were performed with Image Pro Plus software (v. 9.0, Media Cybernetics, Bethesda, MD, U.S.A).

RESULTS

Testis

Overall, spermatogenesis in *N. subnodosus* showed the typical concentric pattern, where less-developed cells occurred toward the tubular periphery and more-developed cells in the center of seminal tubules (Fig. 1). Despite this, the distribution of maturing cells from the lumen to the periphery did not maintain a clear relationship in the testis and with at all developmental stages (Fig. 1).

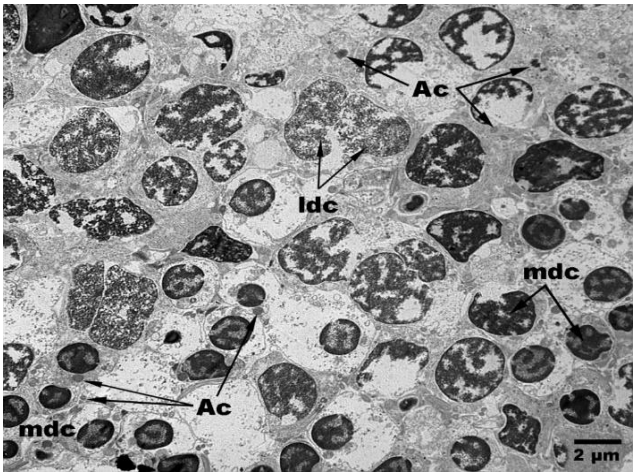

Figure 1. Testis in lion's paw scallop *N. subnodosus* showing larger, less developed cells (ldc) associated with some auxiliary cells (Ac) in the lumen of seminal tubules, as well as smaller, more developed cells (mdc) toward the tubular periphery. Lysis processes with ruptured cell membranes are observed at some sites.

Figura 1. Testículo en la alemeja mano de león *N. subnodosus* mostrando células más grandes y menos desarrolladas (ldc) asociadas con algunas células auxiliares (Ac) en la luz de los túbulos seminales, así como células más pequeñas y más desarrolladas (mdc) hacia la periferia tubular. En algunos sitios se observan procesos de lisis con rotura de membranas celulares.

Spermatogonia

This is the largest cell type of the male germline and is always associated with the basal membrane (Fig. 2a). Spermatogonia are in contact with, or separated by, cytoplasm projections of auxiliary cells; they have a large, round nucleus located centrally, as well as a few heterochromatin granules of different sizes scattered across the nucleoplasm. The clear spaces within the nucleus are abundant and correspond to euchromatin with little percentage of heterochromatin occupancy. In addition to abundant electrodense material, some organelles can be seen, such as the Golgi complex and a variable number of scattered mitochondria measuring 0.33 ± 0.06 μm^2 mean area and 0.58 ±0.12 µm mean length (Figs. 2a, b). At the end of this stage, spermatogonia undergo a rapid process of mitosis in which heterochromatin accumulation significantly increases (Table 2).

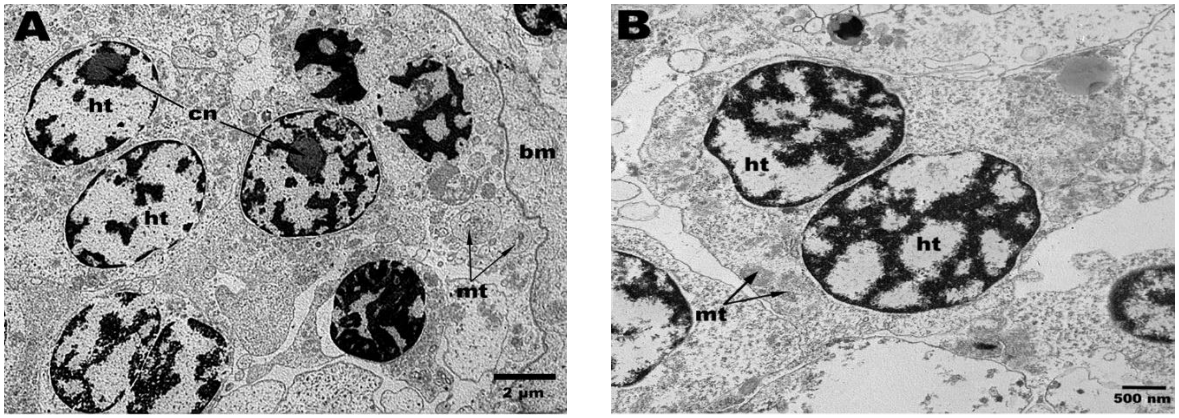

Figure 2. Spermatogonia in mitotic division in lion's paw scallop *N. subnodosus*, showing lax heterochromatin (ht) undergoing mitosis, some central nuclei (cn), and a few mitochondria (mt) scattered in the cytoplasm or near the basal membrane (bm) (A, B).
Figura 2. Espermatogonias en división mitótica en la almeja mano de león *N. subnodosus*, que muestra heterocromatina laxa (ht) en proceso de mitosis, algunos núcleos centrales (cn) y algunas mitocondrias (mt) dispersas en el citoplasma o cerca de la membrana basal (bm) (A, B).

Table 2. Main measurements and characteristics of the different cell types occurring during spermatogenesis of lion's paw scallop *N. subnodosus*.
Tabla 2. Principales mediciones y características de los diferentes tipos celulares que ocurren durante la espermatogénesis de la almeja mano de león *N. subnodosus*.

Cell type	Cell area (μm^2)	Cell length (µm)	Nucleus area (μm^2)	Nucleus length (µm)	Chromatin occupancy
Spermatogonia	38.9 ±4.43	6.41 ±1.94	11.55 ±.33	4.95 ±0.67	Increases from 35% (initially) to 47.9% (at the end)
Primary spermatocyte	15.5 ±1.00	3.81 ±0.39	6.18 ±0.42	2.73 ±0.25	~55 ±0.56%
Secondary spermatocyte	7.48 ±0.10	2.93 ±0.59	2.33 ±0.40	1.68 ±0.28	~68 ±0.45%
Spermatid	2.39 ±0.65	–	2.13 ±0.30	1.64 ±0.26	~90 ±0.31%
Spermatozoon	2.16 ±0.45	–	2.04 ±0.16	1.5 ±0.070	~100%

Primary spermatocyte

Compared to spermatogonia, these cells are characterized by a substantial reduction in size and nucleus size (Figs. 3a, b; Table 2). The cytoplasm-nucleus ratio increases (29.7% of spermatogonia to 39.9% of primary spermatocytes). In the cytoplasm, mitochondria decrease in number, but maintain their size (mean area =0.33 ± 0.06 μm^2; mean length =0.58 ±0.12 µm). The occupancy of condensed heterochromatin in the nucleus is higher, leading to a decrease in the coverage of the clear spaces within (Figs. 3a, b).

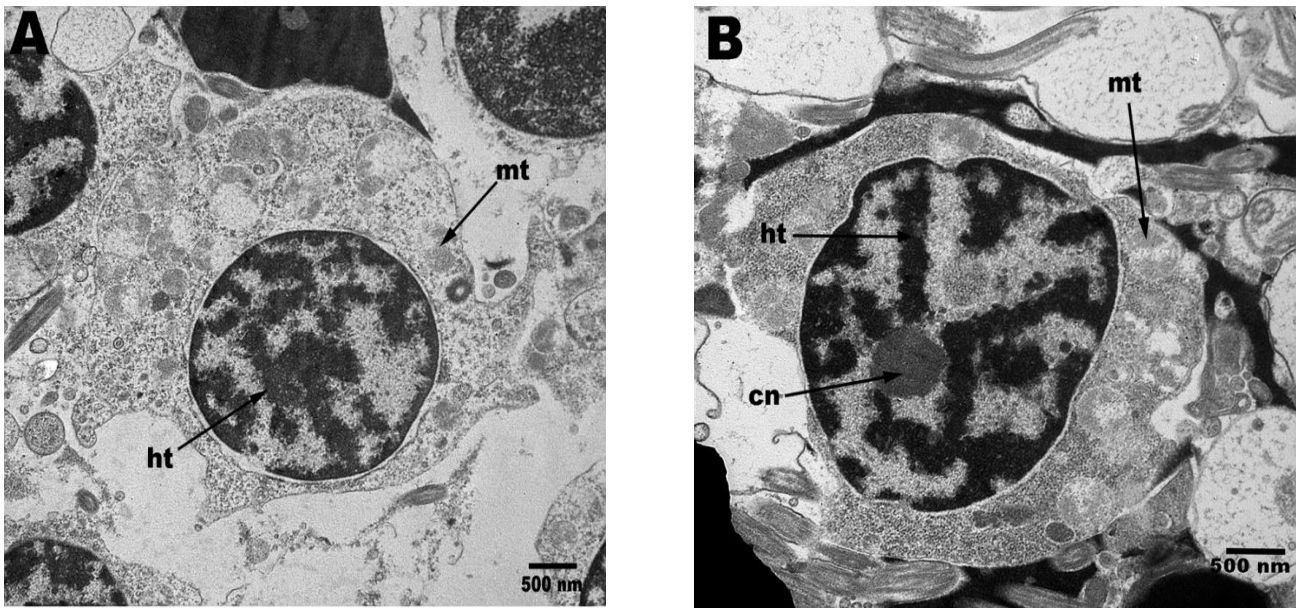

Figure 3. Primary spermatocyte in lion's paw scallop *N. subnodosus*, showing condensed heterochromatin (ht), a central nucleus (cn), and a few mitochondria (mt) starting to align to the still-unformed midpiece (A, B).
Figura 3. Espermatocito primario en la almeja mano de león *N. subnodosus*, que muestra heterocromatina condensada (ht), un núcleo central (cn) y algunas mitocondrias (mt) que comienzan a alinearse con la pieza intermedia aún no formada (A, B).

Secondary spermatocyte

Secondary spermatocytes are rarely observed because of the rapid onset of the second meiotic division. They generally undergo a significant reduction in size and nucleus size (Fig. 4; Table 2). The number of mitochondria decreases again, and while they maintain the same size as the primary spermatocyte, they begin to migrate towards the basal pole. The percentage of heterochromatin condensation also increases (68% ±0.45%) and now acquires a peripheral arrangement in the nucleus and in some part of the lumen, resembling a typical donut (Fig. 4).

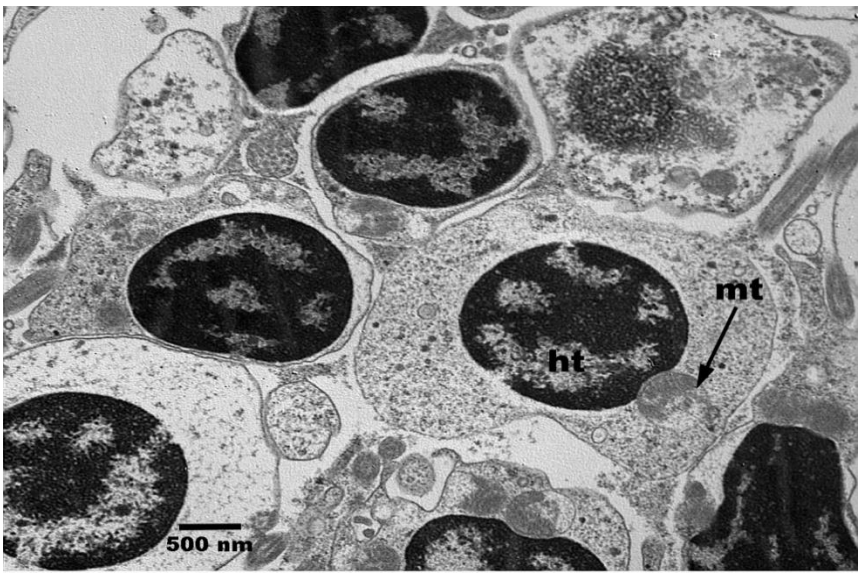

Figure 4. Secondary spermatocyte in lion's paw scallop *N. subnodosus*, showing a high percentage of condensed heterochromatin (ht) and some mitochondria (mt) aligned near the forming midpiece.
Figura 4. Espermatocitos secundarios en la almeja mano de león *N. subnodosus*, mostrando un alto porcentaje de heterocromatina condensada (ht) y algunas mitocondrias (mt) alineadas cerca de la pieza media en formación.

Spermatid

The process of spermiogenesis begins with spherical, or nearly spherical, cells that again decrease in size and have a central smaller nucleus that now occupies most of the cytoplasm (Fig. 5; Table 2). At this stage, four mitochondria of smaller size (mean area = 0.29 ±0.01 μm^2 and mean length =0.64 ±0.05 μm) and spherical shape can be observed near the basal pole (Figs. 5a, b). In spermatids with a high degree of differentiation, the cytoplasm is limited to a thin halo around the nucleus. When visible, the proacrosomal vesicle migrates from the bottom towards the apex of each spermatid, becoming conical, invaginated, and less electrodense at the periphery. Heterochromatin now occupies ~90% of the nucleoplasm.

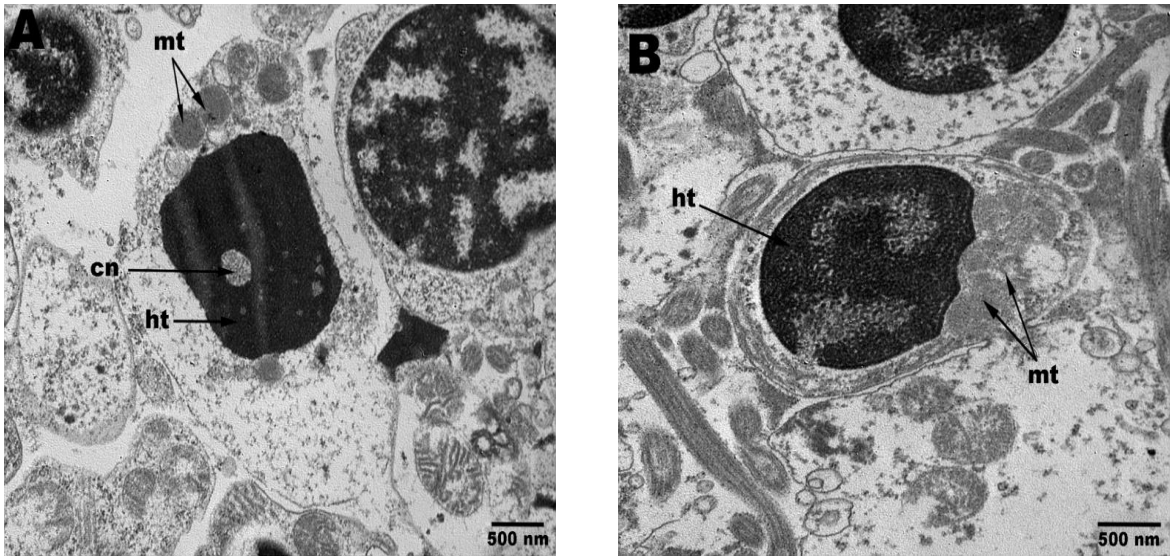

Figure 5. Spermatid in lion's paw scallop *N. subnodosus*, showing highly condensed heterochromatin (ht), a clear, small central nucleus (cn), and four mitochondria (mt) fully aligned to the midpiece (A, B).
Figura 5. Espermátida en la almeja mano de león *N. subnodosus*, mostrando heterocromatina altamente condensada (ht), un núcleo central pequeño y transparente (cn) y cuatro mitocondrias (mt) completamente alineadas con la pieza intermedia (A, B).

Spermatozoon

After the spermiogenesis process, the early sperm cell begins to migrate into the lumen of the seminal tubules and undergoes a complex transformation to form the head, midpiece, and flagellum (Fig. 6a). The acrosome is not always visible at this stage. The nucleus is smaller, becomes bullet-shaped, and the condensed granular heterochromatin now occupies its entire matrix. When near ripe, the sperm acrosome becomes visible, reduces in size (mean length =0.59 ±0.05), and adopts a typically conical shape, being convex towards the apical region and concave towards the nucleus (Fig. 6c). The apical region contains darker electrodense granular material and the region near the nucleus more translucent electrodense material (Fig. 6b). The space between the acrosome and nucleus is now occupied by the acrosomal substance enclosed in a small, oval-shaped subacrosomal vesicle measuring 0.19 ±0.01 μm mean length (Fig. 6c). In addition, four spherical mitochondria measuring 0.29 ±0.01 μm^2 mean area and 0.64 ±0.05 μm mean length with well-developed ridges are clearly visible in the midpiece (Fig. 6d). Sometimes, two lateral satellite fibers appear linked to the distal centriole in the sperm cell. When the flagellum is fully formed, the centriole between the mitochondria adopts the typical 9+2 arrangement of peripheral and central pairs of microtubules (Fig. 7). The mean features of the sperm cell are shown in Table 2.

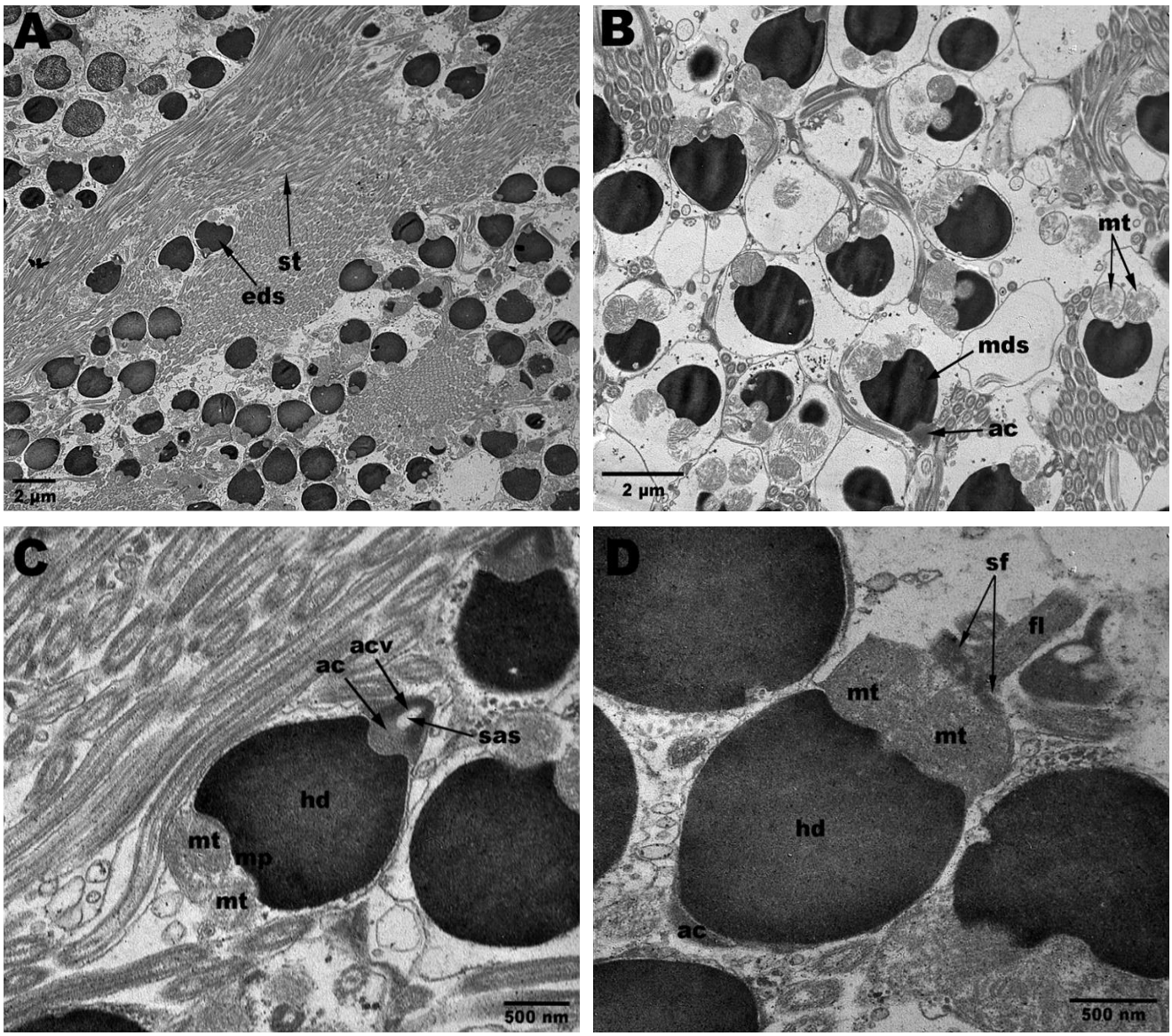

Figure 6. Spermatozoon in lion's paw scallop *N. subnodosus* showing: (A) abundant early-developing sperm cells (eds) with their tails lined-up within the seminal tubules (st); (B) mid-developing sperm cells (mds) with a clear acrosome (ac) and two spherical mitochondria (mt) in the midpiece; (C) near-ripe sperm cell with the head (hd), conical acrosome (ac), oval proacrosomal vesicle (acv), subacrosomal substance (sas), and spherical mitochondria (mt) in the midpiece (mp); and (D) fully-formed sperm cell with two of four visible mitochondria (mt) and two lateral satellite fibers (sf) near the distal centriole and the flagellum (fl).

Figura 6. Espermatozoide en la almeja mano de león *N. subnodosus* mostrando: (A) abundantes espermatozoides de desarrollo temprano (eds) con sus colas alineadas dentro de los túbulos seminales (st); (B) espermatozoides de desarrollo medio (mds) con un acrosoma transparente (ac) y dos mitocondrias esféricas (mt) en la pieza intermedia; (C) espermatozoide casi maduro con cabeza (hd), acrosoma cónico (ac), vesícula proacrosomal ovalada (acv), sustancia subacrosomal (sas) y mitocondrias esféricas (mt) en la pieza media (mp); y (D) espermatozoide completamente formado con dos de las cuatro mitocondrias visibles (mt) y dos fibras satélite laterales (sf) cerca del centríolo distal y el flagelo (fl).

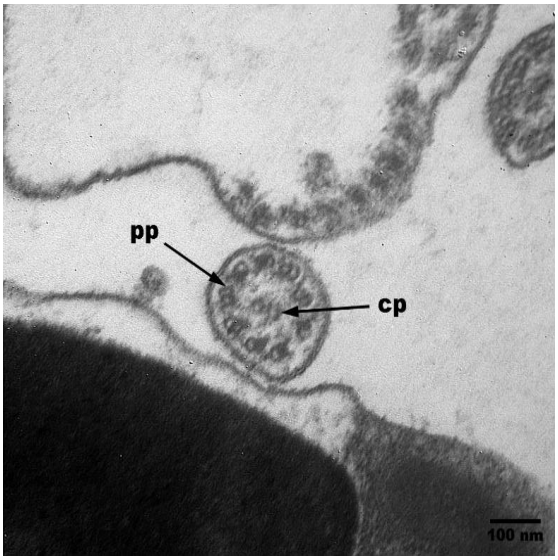

Figure 7. Transversal section of the flagellum in lion's paw scallop *N. subnodosus*, showing the microtubular arrangement of one central pair (cp) and nine peripheric pairs (pp).
Figura 7. Sección transversal del flagelo de la almeja mano de león *N. subnodosus*, mostrando la disposición microtubular de un par central (cp) y nueve pares periféricos (pp).

DISCUSSION

This study is the first to describe the ultrastructure of spermatogenesis in *N. subnodosus* and confirms that the overall concentric arrangement of developing cells, particularly during the spermatogonia to spermatocyte stages, is consistent with the pattern reported for most bivalve species undergoing external fertilization (Frazen 1970, Suwanrajat and Parnrong 1999, Healy *et al.* 2000, Ortíz *et al*. 2003, 2006, Villalejo-Fuerte *et al.* 2018). Some of the similarities include the presence of a primitive-type, tailed sperm cell, four mitochondria at the basal pole, and a 9+2 arrangement of microtubules surrounding the distal centriole. These features also occur in the Yesso scallop *Patinopecten yessoensis*, Atlantic-bay scallop *Argopecten irradians* and Farrer's scallop *Chlamys farreri farreri* (Kim 2001), and Swift's scallop *Chlamys swiftii* (Jun *et al*. 2012). In contrast, the mean sizes of the head, acrosome, and nucleus in *N. subnodosus* are among the smallest within the family Pectinidae, along with those in *A. irradians* (Kim 2001) (see Table 1).

In *N. subnodosus*, the main changes in cell morphology during spermatogenesis occurred at the spermatid and spermatozoa stages. Taxonomically, these changes are important for establishing comparisons between gonochoristic bivalves and hermaphrodite scallops, and for detecting similarities and differences between superfamilies, families, and species (Kim 2001, Jun *et al*. 2012, Kang *et al.* 2012). These comparisons are based on the little variation shown by the midpiece and flagellum in marine bivalves with external fertilization, compared to the large variation in the nucleus and acrosome (Camacho-Mondragón *et al.* 2014). In the family Pectinidae, however, features such as the shape of the nucleus and acrosome, number of mitochondria in the midpiece, and presence of satellite fibers linked to the distal centriole are similar for many species (Kim 2001, Jun *et al*. 2012). Clearly, the bullet-type nucleus and conical acrosome of *N. subnodosus* is consistent with the overall pattern described for the scallops *P. yessoensis*, *A. iiradians*, and *C. farreri farreri* (Table 1). In gonochoristic bivalves, in contrast, the nucleus and acrosome may adopt different shapes, but maintaining a stable pattern between families, superfamilies, and species (Franzen 1970; Healy *et al*. 2000). For example, the sperm nucleus is spherical in *A. tuberculosa* (Ortíz *et al*. 2003), *A. maura* (Camacho-Mondragón *et al*. 2014), and *S. calcifer* and *S. princeps* (Villalejo-Fuerte *et al.* 2018); it is ovoid in *C. californiensis* (Ortíz *et al.* 2006) and *A. pectinata* (Kang *et al.* 2012), and cylindrical in *R. philippinarum* (Kim *et al.* 2013). On the other hand, the acrosome is conical in *A. pectinata* (Kang *et al*. 2012), *A. maura* (Camacho-Mondragón *et al*. 2014), and *S. calcifer* and *S. princeps* (Villalejo-Fuerte *et al*. 2018); it is a modified cone in *R. philippinarum* (Kim *et al*. 2013), a pyramid in *A. tuberculosa* (Ortíz *et al*. 2003), and a sphere in *C. californiensis* (Ortíz *et al.* 2006).

In the sperm stage, both the conical acrosome and oval proacrosomal vesicle are small in *N.. subnodosus*. Interestingly, these structures are also small in *P. yessoensis* and *A. irradians*, but are large in *C. swiftii* and *C. farreri farreri* (Kim 2001, Jun *et al*. 2012) (Table 1). We also noted that the proacrosomal vesicle formed until the sperm stage, in contrast to the early formation of this structure from the spermatocyte stage in *C. virginica* (Eckelbarger and Davis, 1996) and *A. maura* (Camacho-Mondragón *et al*. 2014) and the spermatid stage in *P. maximus* (Dorange and Le Pennec, 1989) and *R. philipinarum* (Kim *et al*. 2013). These differences indicate that the mechanisms responsible for acrosome formation and maturation are not completely understood in the family Pectinidae, although they have taxonomic importance. This is also the case for the subacrosomal substance, which in nearly ripe spermatozoa is composed of both darker electrodense material toward the apical region and more translucent electrodense material toward the nucleus. Chemically, this substance contains different types of hydrolytic enzymes that facilitate penetration and fertilization of the egg. Thus, it is likely that differences in chemical composition of this substance reflect species-specific energy demands by the sperm to ensure both biological processes (Franzen 1970, Healy 1995, Healy *et al*. 2000, Kang *et al*. 2012).

Suwanrajat and Parnrong (1999) argued that the number of mitochondria in the midpiece is another feature of current taxonomic value in the class Bivalvia, given the differences observed among families and even among species of the same family. For instance, while four mitochondria are observed in the white clam *C. californiensis* (Ortiz *et al*. 2006), the penshell *A. maura* (Camacho-Mondragón *et al*. 2014), and the scallops *P. yessoensis*, *C. farreri farreri*, *C. swiftii*, and *N.. subnodosus* (Kim 2001; present study), other species such as the black ark *A. tuberculosa* and the Atlantic-bay scallop *A. irradians irradians* have five mitochondria (Kim 2001, Ortíz *et al*. 2003). Furthermore, Villalejo-Fuerte *et al*. (2018) found up to seven large mitochondria forming a ring at the posterior part of the spermatozoon in *S. princeps* (Table 1). In general, most studies agree that the number of mitochondria in the midpiece is stable at the family level, and although authors such as Healy *et al*. (2000), Jun *et al*. (2012), Kang *et al*. (2012) and Kim *et al*. (2013) report five of them for the family Pinnidae, Camacho-Mondragón *et al*. (2014) only observed four in *A. maura*. These differences in the number of mitochondria may denote a simplification and possible evolutionary derivation from the basic type of ect-aquasperma' (Healy *et al*. 2000, Kang *et al*. 2012), but may also reflect species-specific energy needs of the flagellum to displace in different types of aquatic environments (*e.g.* oligotrophic or heterotrophic) and ensure fertilization (Camacho-Mondragón *et al*. 2014).

Similar to the proacrosomal vesicle, the flagellum formed until the spermatozoon stage in *N. subnodosus*, when it usually develops from the primary spermatocyte or spermatid stages in other bivalve species with external fertilization (Franzen 1970; Suwanrajat and Parnrong 1999, Kang *et al*. 2012, Camacho-Mondragón *et al*. 2014). When fully ripe, three patterns of the sperm cell were evident in *N. subnodosus*: (1) the typical 9+2 arrangement of microtubules surrounding the centriole; (2) the maximum condensation of heterochromatin (>90%) to comply with the high synthetic activity of ribonucleic proteins that ensure full maturation of the spermatozoa (Dimitri *et al*. 2009, Kang *et al*. 2012); and (3) the presence of two lateral satellite fibers linked to the distal centriole, which in terms of motility, provide a mechanical advantage to the sperm by increasing the integrity and resistance of the flagellum. The presence of satellite fibers is common among the Pectinidae and has been confirmed in *P. yessoensis*, *C. farreri farreri*, and *A. irradians irradians* (Kim 2001, Jun *et al*. 2012, Kang *et al*. 2012). These structures have also been found in the Ostreidae, Mytilidae, and Arcidae families (Jun *et al*. 2012), but the selective pressures defining the similarities or differences among families, superfamilies, and species have not been satisfactorily explained (Healy *et al*. 2000, Kim 2001, Jun *et al*. 2012; Camacho-Mondragón *et al*. 2014).

In conclusion, we identified three morphological features that are stable within the Pectinidae and have taxonomic value in *N. subnodosus*: (1) the bullet-type nucleus, conical acrosome, and small oval proacrosomal vesicle that formed up to the sperm stage, along with the flagellum; (2) the appearance of four spherical mitochondria in the midpiece; and (3) the presence of two satellite fibers near the distal centriole. These evidences suggest that *N. subodosus* may be more closely-related to *P. yessoensis*, *C. farreri farreri*, *C. swiftii*, and *A. irradians* within the family Pectinidae than to any other bivalve family. As a strategy to broaden the understanding of the reproductive strategy and life cycle of this species, characterization of the ultrastructure of oogenesis is ongoing.

Declaration of conflict of interest

The authors declare no conflict of interests

Declaration of good practices with animals

The animals were subjected to experimentation according to the management and care plan for CONACYT, Mexico.

ACKNOWLEDGMENTS

The authors are grateful to Sociedad Cooperativa de Bahía Tortugas, in Bahía Tortugas, Baja California Sur, for donating the scallops used in this study. We also wish to thank Horacio Bervera, Juan José Ramírez, and Enrique Calvillo (at CIBNOR) for field support during collection and transportation of scallops. Diana Dorantes provided English editorial services. This study was part of the M.Sc. thesis prepared by M.A.A.D. (CONACYT #297361) and was funded by Consejo Nacional de Ciencia y Tecnología (CONACYT grant #078C leaded by P.E.S.) and Secretaría de Investigación y Posgrado (SIP grant #20101187 leaded by M.A.M.).

REFERENCES

Angel-Dapa M.A., Arellano-Martínez M., Ceballos-Vázquez B.P., Acosta-Salmón H., Saucedo, P.E. (2015). Comparative analysis of the reproductive strategy of lion's paw scallop *Nodipecten subnodosus* in Baja California Sur, Mexico. Lat Am J Aquatic Res. 43: 616–620.

Arellano-Martínez M., Ceballos-Vázquez B.P., Villalejo-Fuerte M., García-Domínguez F., Elorduy-Garay J.F., Esliman-Salgado A., Racotta, I.S. (2004a). Reproduction of the lion's paw scallop *Nodipecten subnodosus* Sowerby, 1835 (Bivalvia: Pectinidae) from Laguna Ojo de Liebre, B.C.S., Mexico. J Shellfish Res. 23: 723–729.

Arellano-Martínez M., Racotta I.S., Ceballos-Vázquez B.P., Elorduy-Garay J.F. (2004b). Biochemical composition, reproductive activity and food availability of the lion's paw scallop *Nodipecten subnodosus* in the Laguna Ojo de Liebre, Baja California Sur, Mexico. J Shellfish Res. 23: 15–23.

Beltrán-Lugo A.I., Maeda-Martínez A., Pacheco-Aguilar R., Nolasco-Soria H. (2006). Seasonal variations in chemical, physical, textural, and microstructural properties of adductor muscles of Pacific lions-paw scallop (*Nodipecten subnodosus*). Aquaculture 258: 619–632.

Camacho-Mondragón M.A., Ceballos-Vázquez B.P., Uría-Galicia E., López-Villegas E.O, Arellano-Martínez M. (2014). Ultraestructure of the spermatogenic process in the penshell *Atrina maura* (Bivalvia: Pinnidae). Malacologia 57: 329–339.

De Gaulejac B., Henry M., Vicente N. (1995). An ultrastructural study of gametogenesis of the marine bivalve *Pinna nobilis* (Linnaeus 1758). II. Spermatogenesis. J. Mollusc Stud. 61: 393–403.

Dimitri P., Caizzi R., Giordano E., Accardo M.C., Lattanzi G., Biamonti G. (2009). Constitutive heterochromatin: a surprising variety of expressed sequences. Chromosoma 118: 419–435.

Dorange G. and Le Pennec M. (1989). Ultrastructural characteristics of spermatogenesis in *Pecten maximus* (Mollusca, Bivalvia). Invert Repro Dev. 15: 109–117.

Eckelbarger K.J. and Davis C.V. (1996). Ultrastructure of the gonad and gametogenesis in the eastern oyster, *Crassostrea virginica*. II. Testis and spermatogenesis. Mar Biol. 127: 89–96.

Franzen A. (1970). Phylogenetic aspects of the morphology of spermatozoa and spermiogenesis. In: Baccetti, B., Karp, G., Berrill, N.J. (eds.), Comparative Spermatology. McGraw-Hill, New York, pp. 3–46.

Gutiérrez-Villaseñor C.E., Chi-Barragán G. (1997). Effect of temperature and feeding ratio on the conditioning of *Lyropecten subnodosus* (Sowerby, 1835). In: Book of Abstracts. *Proceedings 11th International Pectinid Workshop, CICIMAR*, La Paz, Baja California Sur, Mexico, pp. 73–75.

Healy J.M. (1995). Spermatozoa and spermatogenesis in a monoplacophoran mollusk, *Leavipilina antartica*: ultrastructure and comparison with other Mollusca. Mar. Biol. 122: 53-65.

Healy J.M., Keys J.L., Daddow L.Y.M. (2000). Comparative sperm ultrastructure in pteriomorphian bivalves with special reference to phylogenetic and taxonomic implications. In: Harper, E.M., Taylor, J.D., Crame, J.A. (eds.), The evolutionary Biology of the Bivalvia. Special Publications Geological Society, London, UK, pp. 169–190.

Jun J.C, Kim J.H., Park Y.J., Kang H.W., Chung J.S., Chung E.Y. (2012). Morphology and taxonomic values of the sperm in male *Chlamys* (*Swiftopecten*) *swiftii* (Pteriomorphia: Pectinidae) in Western Korea. Korean J. Malacol. 28: 165–174.

Kang H.W., Chung E.Y., Kim J.H., Chung J.S., Lee K.Y. (2012). Germ cell differentiations during spermatogenesis and taxonomic values of mature sperm morphology of *Atrina (Servatrina) pectinata* (Bivalvia, Pteriomorphia, Pinnidae). Dev Repro. 16: 19–29.

Kim J.H. (2001). Spermatogenesis and comparative ultrastructure of spermatozoa in several species of Korean economic bivalves (13 families, 34 species). Ph.D. Thesis, Pukyung National University, Daeyeon, South Korea.

Kim J.H., Chung J.S., Lee K.Y. (2013). Ultraestructural characteristics of the testis, spermatogenesis and taxonomic values of sperm morphology in male *Ruditapes philippinarum* in Western Korea. Dev Repro. 17: 121–132.

López-Sánchez J.A., Maeda-Martínez A.N., Croll R.P., Acosta-Salmón H. (2009). Monoamine fluctuations during the reproductive cycle of the Pacific lion's paw scallop *Nodipecten subnodosus*. Comp Biochem Physiol. A. 154: 425–428.

Maeda-Martínez A.N. and Lodeiros C. (2011). Biología y cultivo de moluscos pectinidos del género *Nodipecten*. Ed. Limusa, México City, 398 p.

Ortíz E., Uría-Galicia E., Silva-Olivares A., Tsutsumi V., Shybayama M. (2003). Estudio de la ultraestructura de la espermatogénesis de *Anadara tuberculosa* (Sowerby, 1833) (Mollusca: Pelicipoda: Arcidae). Hidrobiológica 13: 145–150.

Ortíz E., Uría-Galicia E., Silva-Olivares A., Tsutsumi V., Shybayama M. (2006). Ultraestructure of spermatogenesis in the white clam *Chione californiensis* (Broderip, 1835) (Mollusca: Pelecipoda). J Shellfish Res. 25: 399–401.

Palacios E., Racotta I.S., Kraffe E., Marty Y., Moal J., Samain J.F. (2005). Lipid composition of the giant lion's paw scallop (*Nodipecten subnodosus*) in relation to gametogenesis: I. Fatty acids. Aquaculture 250: 270–282.

Palacios E., Racotta I.S., Arjona O., Marty Y., Coz J.R., Moal J., Samain J.F. (2007). Lipid composition of the pacific lion's paw scallop, *Nodipecten subnodosus*, in relation to gametogenesis. 2. Lipid classes and sterols. Aquaculture 266: 266–273.

Suwanrajat J. and Parnrong S. (1999). Reproductive cycles of *Anadara granosa* L. in Jebilung Satun Province. Warasan Songkhanakarin 12: 341–351.

Thielley M., Weppe M., Herbaut C. (1993). Ultrastructural study of gametogenesis in the French Polynesian black pearl oyster *Pinctada margaritifera* (Mollusca, Bivalvia). I. Spermatogenesis. J Shellfish Res. 12:41–47.

Villalejo-Fuerte M., Camacho-Mondragón M.A., Ceballos-Vázquez B.P., López-Villegas E.O., Uría-Galicia E., Arellano-Martínez M. (2018). Ultrastructure of sperm development and mature sperm morphology in *Spondylus calcifer* and *S. princeps* (Bivalvia: Spondylidae). Malacologia 62: 1–10.